

# Magnetic dissipation in the Crab nebula

Serguei S. Komissarov

*Department of Applied Mathematics, The University of Leeds, Leeds, LS2 9GT, UK*  
*E-mail: serguei@maths.leeds.ac.uk*

Received/Accepted

## ABSTRACT

Magnetic dissipation is frequently invoked as a way of powering the observed emission of relativistic flows in Gamma Ray Bursts and Active Galactic Nuclei. Pulsar Wind Nebulae provide closer to home cosmic laboratories which can be used to test the hypothesis. To this end, we reanalyze the observational data on the spindown power of the Crab pulsar, energetics of the Crab nebula, and its magnetic field. We show that unless the magnetic inclination angle of the Crab pulsar is very close to 90 degrees the overall magnetization of the striped wind after total dissipation of its stripes is significantly higher than that deduced in the Kennel-Coroniti model and recent axisymmetric simulations of Pulsar Wind Nebulae. On the other hand, higher wind magnetization is in conflict with the observed low magnetic field of the Crab nebula, unless it is subject to efficient dissipation inside the nebula as well. For the likely inclination angle of 45 degrees the data require magnetic dissipation on the timescale about 80 years, which is short compared to the life-time of the nebula but long compared to the time scale of Crab’s gamma-ray flares.

**Key words:** ISM: supernova remnants – MHD – magnetic fields – radiation mechanisms: non-thermal – relativity – pulsars: individual: Crab

## 1 INTRODUCTION

Magnetic fields are often invoked in models of the relativistic jet production by central engines of Active Galactic Nuclei (AGN) and Gamma Ray Bursts (GRB). In these theories the jets are Poynting-dominated at the origin, with the magnetization parameter  $\sigma = B^2/4\pi\rho c^2 \gg 1$ . This is different from the earlier essentially hydrodynamic, low  $\sigma$ , models of relativistic jets in one important aspect. Even strong, high Mach number shocks, in high  $\sigma$  plasma are weakly dissipative compared to their low  $\sigma$  counterparts (e.g. Kennel & Coroniti 1984a; Komissarov 2012). Moreover, PIC simulations show that the acceleration of nonthermal particles may also be problematic at such shocks (Sironi & Spitkovsky 2009, 2011a). This suggests that either the Poynting flux is first converted into the bulk motion kinetic energy via ideal MHD mechanism (e.g. Vlahakis & Königl 2004; Komissarov et al. 2009; Lyubarsky 2010), which is then dissipated at shocks, or the magnetic energy is converted directly into the energy of emitting particles via magnetic dissipation, which accompanies magnetic reconnection events (e.g. Drenkhahn & Spruit 2002; Lyutikov & Blandford 2003; Zhang & Yan 2011; Giannios 2011; McKinney & Uzdensky 2012). In fact, the magnetic dissipation can facilitate bulk acceleration of jets as well (e.g. Drenkhahn & Spruit 2002).

While AGN and GRBs are very distant sources, which makes their observational studies rather difficult, there exist

objects much “closer to home” which share similar properties, the Pulsar Wind Nebulae (PWN). They are powered by relativistic winds from neutron stars and these winds are also expected to be Poynting-dominated at their base (see Arons 2012, and references therein). In particular, the Crab nebula is one of the brightest sources of nonthermal emission in the sky throughout the whole observational range of photon energies. Its large angular size (of seven arc minutes), ensures that its spatial structure is well resolved and its relatively small linear size (of several light years) allows direct observations of not only its small-scale structural variability but also its overall dynamics. Because the Crab nebula is such an easy object to observe it has been studied with the level of detail which may never be reached in observations of AGN and GRB jets, and it is rightly considered as a testbed of relativistic astrophysics.

The early attempts to build a theoretical model of the Crab nebula using the ideal relativistic MHD approximation resulted in a paradoxical conclusion that the pulsar wind has to have  $\sigma \sim 10^{-3}$  near its termination shock (Rees & Gunn 1974; Kennel & Coroniti 1984a; Emmering & Chevalier 1987; Begelman & Li 1992). A slightly higher magnetization,  $\sigma \sim 10^{-2}$ , was later suggested by axisymmetric numerical simulations (Komissarov & Lyubarsky 2003; Del Zanna et al. 2004; Bogovalov et al. 2005), although no proper study of this issue has been carried out. The key property of these analytical and numerical solutions is their purely

arXiv:1207.3192v3 [astro-ph.HE] 15 Oct 2012

toroidal magnetic field. The strong hoop stress of such field creates excessive axial compression of the nebula in solutions with higher  $\sigma$  and pushes the termination shock too close to the pulsar in the Kennel-Coroniti model, in conflict with the observations. On the other hand, the ideal relativistic MHD acceleration of uncollimated wind-like flows is known to be very inefficient, leaving such flows Poynting-dominated on the astrophysically relevant scales (e.g. Lyubarsky 2011; Komissarov 2011). This striking conflict is known as the  $\sigma$ -problem.

Attempts have been made to see if  $\sigma$  can be reduced via magnetic dissipation in the so-called striped zone of pulsar winds, where the magnetic field changes its polarity on the length scale  $\lambda_p = cP$ , where  $P$  is the pulsar period (Coroniti 1990; Lyubarsky & Kirk 2001). The dissipation is accompanied by the wind acceleration via conversion of the thermal energy into the bulk kinetic energy of the flow during its adiabatic expansion. Unfortunately, for the wind of the Crab pulsar the dissipation length scale significantly exceeds the radius of the wind termination shock, thus making this mechanism inefficient (Lyubarsky & Kirk 2001).

Lyubarsky (2003b) has demonstrated that the energy associated with the alternating component of magnetic field of the striped wind can be rapidly dissipated at the termination shock itself, where the characteristic Larmor radius of shock-heated plasma exceeds the wavelength of magnetic stripes. His solution of the shock equations, which accounts for the “erasing” of stripes, shows that the post-shock flow is the same as it would be if the dissipation had already been fully completed in the wind. Sironi & Spitkovsky (2011b) have used 3D PIC simulations to study the magnetic dissipation and particle acceleration at the termination shock of the striped wind numerically and concluded that efficient magnetic dissipation occurs even when the Larmor radius remains below the stripes wavelength, via rapid development of the tearing mode instability and magnetic reconnection in the post-shock flow.

One way or another, this dissipation occurs only in the striped zone and only the alternating component of magnetic field dissipates. Outside of the striped zone, around the poles, the pulsar wind  $\sigma$  remains unaffected by this dissipation and hence very high. As the result, the overall magnetization of plasma injected into the nebula can be much higher than that of the Kennel-Coroniti model, unless the striped zone spreads over almost the entire wind (Coroniti 1990).

Lyubarsky (2003a) argued that in the polar zone the wind  $\sigma$  can be reduced via the flow acceleration accompanying dissipation of fast magnetosonic waves emitted by the pulsar into the polar zone. However, it seems unlikely that the energy flux associated with these waves can dominate the wind energetics in the polar zone. At least, the 3D numerical simulations of pulsar winds (A.Spitkovsky, private communication) show that their contribution is rather small. Thus, we do not expect  $\sigma$  of the polar zone to be below unity.

An alternative solution to the  $\sigma$  problem has been proposed by Begelman (1998), who argued that the axial compression of the nebula can be reduced via the current-driven kink instability, resulting in more or less uniform total pressure distribution inside the nebula. This would make the overall structure and dynamics of the nebula similar to those in the models with particle-dominated ultra-relativistic pul-

sar wind. The recent computer simulations of the non-linear development of the kink instability of relativistic z-pinch configurations support this conclusion (Mizuno et al. 2009, 2011). In this scenario, PWN are supplied with highly magnetized plasma, making magnetic dissipation a potentially important process in their evolution and emission.

In this paper, we test whether the magnetic dissipation inside PWN is consistent with the observations of the Crab nebula and its pulsar. The main idea is very simple. First, the timing observations of the Crab pulsar allow us to estimate how much energy has been pumped into the nebula. Second, using the stripe wind model we can calculate how much of this energy is supplied in the magnetic form. Third, a simple dynamical model of the nebula expansion can be used to predict how much magnetic energy is retained by the nebula after adiabatic losses. Finally, the observations of the Crab nebula tell us how much magnetic energy is actually in there and whether the magnetic dissipation is actually required to make the ends meet.

## 2 OVERALL ENERGETICS OF THE CRAB NEBULA

In the simplest approximation, the spindown of pulsars is described by the equation  $\dot{\Omega} \propto -\Omega^n$ , where  $\Omega$  is the pulsar angular frequency and  $n$  is the so-called braking index. This form of the spindown law originates from the magnetodipole vacuum radiation mechanism which gives  $n = 3$ . Force-free (or magnetodynamic) models of pulsar magnetospheres yield the same dependence on  $\Omega$  (Spitkovsky 2006; Kalapotharakos & Contopoulos 2009). Timing observations of pulsars allow to measure the braking index and it turns out to be noticeably lower compared to the value predicted by these simple models (Lyne et al. 1993). The reason for this discrepancy is not established yet, but the spindown law itself seems to be consistent with the observations and we will accept it in our calculations.

The solution to this equation is

$$\Omega = \Omega_0 \left(1 + \frac{t}{\tau}\right)^{-\frac{1}{n-1}}. \quad (1)$$

The corresponding spindown luminosity is

$$L_{sp} = -I\Omega\dot{\Omega} = L_0 \left(1 + \frac{t}{\tau}\right)^{-\frac{n+1}{n-1}}, \quad (2)$$

where  $\tau$  is called the spindown time (Rees & Gunn 1974). From the timing observations of the Crab pulsar,  $n = 2.51$  and  $\tau \simeq 703$  yr (Lyne et al. 1993). For the usually accepted moment of inertia of neutron stars  $I = 10^{45}$  g cm<sup>2</sup>, these measurements imply the current spindown power  $L_{sp} \simeq 4.6 \times 10^{38}$  erg/s and the initial power  $L_0 \simeq 3.3 \times 10^{39}$  erg/s. The corresponding total extracted rotational energy of the Crab pulsar is

$$E = L_0 \tau \frac{n-1}{2} \left(1 - \left(1 + \frac{t}{\tau}\right)^{-\frac{2}{n-1}}\right) \simeq 3.7 \times 10^{49} \text{ erg}, \quad (3)$$

which is 67 percent of its initial rotational energy. The integrated radiative luminosity of the Crab nebula  $L_n \simeq 1.3 \times 10^{38}$  erg/s (Hester 2008) is significantly below  $L_{sp}$ .

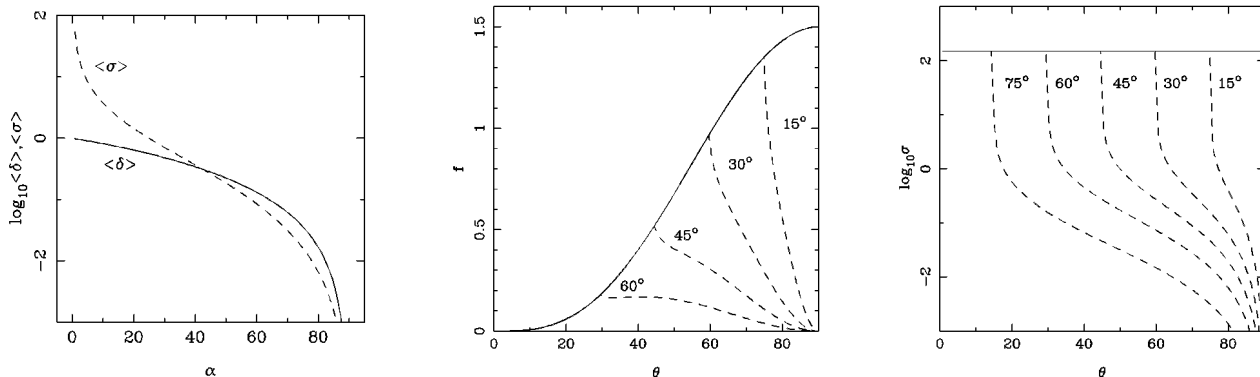


**Figure 1.** *Left panel:* Mean magnetization  $\langle\sigma_\alpha\rangle$  of the pulsar wind after dissipation of its stripes and the mean fraction  $\langle\delta_\alpha\rangle$  of magnetic magnetic energy injected into PWN as functions of the pulsar magnetic inclination angle. *Middle panel:* The distribution of magnetic energy injected into PWN over the polar angle,  $f_\alpha(\theta) = (3/2)\delta_\alpha(\theta)\sin^3\theta$ , for the magnetic inclination angle  $\alpha = 0^\circ$  (solid line)  $15^\circ, 30^\circ, 45^\circ, 60^\circ$  (dashed lines). *Right panel:* The magnetization of the striped wind after dissipation of its stripes as a function of the polar angle for the magnetic inclination angle  $\alpha = 0^\circ$  (solid line),  $15^\circ, 30^\circ, 45^\circ, 60^\circ, 75^\circ$  (dashed lines).

Thus, a large fraction of  $E$  is converted into the kinetic energy of the supernova shell and the internal energy of the PWN, the actual proportion being dependent on the dynamic evolution of the nebula.

Since  $\tau$  is comparable to the current age of the nebula, its global dynamics cannot be described by self-similar models. This forces us to make a number of strong simplifying assumptions in order to render the problem treatable. First, we assume that the nebula is uniform. Second, that the magnetic field becomes randomized, via development of instabilities, and behaves as gas with ultrarelativistic ratio of specific heats  $\Gamma = 4/3$ . In this case, the internal energy of PWN is  $E_n = 3pV$ , where  $p$  is the PWN uniform total pressure and  $V$  is its volume. Third, that the nebula expands with constant speed, and hence  $V \propto t^3$ , which is supported by the rather slow observed acceleration of the nebula (Trimble 1968; Wyckoff & Murray 1977; Bietenholz et al. 1991). Finally, we will ignore its radiative cooling<sup>1</sup>. Under these assumptions the evolution of the internal energy of the nebula is described by the equation

$$\dot{E}_n = L_{sp} - \frac{E_n}{t}, \quad (4)$$

where the last term describes adiabatic cooling. Given the expression (2) for  $L_{sp}$ , the initial condition  $E_n(0) = 0$ , and assuming  $n < 3$ , we find the solution to this equation

$$E_n = \frac{L_0\tau}{a^2 - 3a + 2} \frac{1}{x} \left( 1 - \frac{(a-1)x^2 + ax + 1}{(x+1)^a} \right), \quad (5)$$

where  $a = (n+1)/(n-1)$  and  $x = t/\tau$ . For the parameters of the Crab pulsar, this yields  $E_n \simeq 1.3 \times 10^{49}$  erg. The corresponding spindown energy converted into the kinetic energy of the supernova shell is then  $E_k \simeq 2.4 \times 10^{49}$  erg. The observations indicate that the expansion velocity of the thermal filaments of the Crab nebula increased by 100-200

km/s during the nebula lifetime, which corresponds to increase of their kinetic energy by  $E_k \simeq 10^{49}$  erg (Hester 2008). This agrees rather well with the prediction of our model.

The internal energy  $E_n$  is distributed between the relativistic particles and the magnetic field. The actual partition is dictated by the properties of the pulsar wind, which determine how much energy is injected into the nebula in the magnetic form, and by the interaction between these two components inside the nebula. This interaction can have a reversible form, via the Lorentz force, and an irreversible form, e.g. via magnetic reconnection, collisionless wave dumping and particle acceleration. If the magnetic field is indeed significantly randomized, as we have assumed above, and the Lorentz force is reduced to the magnetic pressure then the reversible interaction is likely to be weak. As a first approximation, we will assume that the irreversible interaction is also weak, in which case the energy distribution between particles and magnetic fields in the nebula equals to that immediately downstream of the termination shock. By comparing the outcome with the observational data, we will be able to say how bad this assumption is and to gauge the importance of magnetic dissipation.

### 3 THE MAGNETIC POWER OF STRIPED WIND

In order to estimate the fraction of the wind energy injected into the nebula in the magnetic form we will employ the split-monopole model by Bogovalov (1999) and the finding of Lyubarsky (2003b) that the overall effect of the stripes dissipation at the termination shock is equivalent to their dissipation upstream of the shock.

Let us denote the angle between the spin axis and the magnetic axis of the pulsar, the magnetic inclination angle, as  $\alpha$ , the angle between the rotation axis and selected streamline of the wind as  $\theta$ , and the phase of the stripe wave as  $\phi$ , with  $\phi = 0$  corresponding to the middle of the stripe with positive (or negative)  $B_\phi$ . Then the phases separating

<sup>1</sup> The radiative cooling would reduce the energy of relativistic particles  $E_e$ , making it even smaller compared to the magnetic energy  $E_m$  than in our calculation. Ultimately, this would make the case for magnetic dissipation even stronger.

the positive and negative stripes are  $\phi_\alpha(\theta)$  and  $2\pi - \phi_\alpha(\theta)$  where

$$\cos \phi_\alpha(\theta) = -\cot(\alpha) \cot(\theta).$$

The conservation of total magnetic flux corresponding to one wavelength allows us to find the magnitude of magnetic field after complete dissipation of its stripes as

$$B = B_0 \begin{cases} |2\phi_\alpha(\theta)/\pi - 1|, & \pi/2 - \alpha < \theta < \pi/2 \\ 1, & \theta \leq \pi/2 - \alpha \end{cases},$$

where  $B_0$  is the magnitude of the magnetic field of the striped wind (In Lyubarsky (2003b),  $B$  is called the mean magnetic field of the striped wind). In these calculations we assume that after completion of this dissipation, the relic current sheets collapse following their adiabatic cooling. The fraction of wind power remaining in the form of Poynting flux along the stream line with the polar angle  $\theta$  is

$$\chi_\alpha(\theta) = \begin{cases} (2\phi_\alpha(\theta)/\pi - 1)^2, & \pi/2 - \alpha < \theta < \pi/2 \\ 1, & \theta \leq \pi/2 - \alpha \end{cases}. \quad (6)$$

Neglecting the small initial contribution of the bulk kinetic energy to the wind power (due to the ideal MHD acceleration in the wind), the wind magnetization along the stream line after the dissipation is

$$\sigma_\alpha(\theta) = \frac{\chi_\alpha(\theta)}{1 - \chi_\alpha(\theta)}.$$

We define the mean magnetization of the wind,  $\langle \sigma_\alpha \rangle$ , as the ratio of its total Poynting flux to its total bulk kinetic energy flux. Since in the split monopole model the energy flux density varies with  $\theta$  like  $\sin^2 \theta$ ,

$$\langle \sigma_\alpha \rangle = \frac{\langle \chi_\alpha \rangle}{1 - \langle \chi_\alpha \rangle}, \quad (7)$$

where

$$\langle \chi_\alpha \rangle = \int_0^{\pi/2} \chi_\alpha(\theta) \sin^3 \theta d\theta.$$

This mean magnetization is shown in the left panel of Figure 1. One can see that unless the pulsar is almost an orthogonal rotator its value is much higher compared to  $\langle \sigma \rangle \simeq 10^{-3}$  of the Kennel-Coroniti model and the values utilized in the 2D numerical simulations,  $\langle \sigma \rangle \simeq 10^{-2}$  (Komissarov & Lyubarsky 2003; Del Zanna et al. 2004; Bogovalov et al. 2005; Camus et al. 2009). Unfortunately,  $\alpha$  is poorly constrained from observations. Using as a guide the value obtained from fitting the spectrum and pulse profile of the high energy emission of the Crab pulsar,  $\alpha \simeq 45^\circ$  (Harding et al. 2008), we obtain  $\langle \sigma \rangle \simeq 0.26$ . Thus, the dissipation of magnetic stripes is apparently unable to resolve the  $\sigma$ -problem completely. This shortcoming of the striped wind model has already been pointed out in Coroniti (1990).

The left panel of Figure 1 shows the distribution of  $\sigma$  over the polar angle, where its value outside of the striped zone is artificially limited by the rather arbitrary value of  $\sim 100$ . In reality, this value should be determined by the

**Table 1.**

$\alpha$	$10^\circ$	$20^\circ$	$30^\circ$	$40^\circ$	$50^\circ$	$60^\circ$	$70^\circ$	$80^\circ$
$\langle \delta_\alpha \rangle$	0.82	0.64	0.48	0.34	0.23	0.13	0.061	0.017

dissipation of fast magnetosonic waves emitted by the pulsar (Lyubarsky 2003a). However, the efficiency of this emission in 3D numerical simulations of dipolar pulsar magnetospheres seems to be rather low and thus one would indeed expect a rather high magnetization in the polar region.

Next we consider the plasma compression at the termination shock of such a wind. The magnetic flux conservation ensures that at the shock  $Bv_n = \text{const}$ , where  $v_n$  is the normal component of velocity. This implies that downstream of the shock the Poynting flux is increased by the shock compression factor  $\eta = v_{n,1}/v_{n,2}$ . In the case of strong ultrarelativistic shock,

$$\eta(\chi) = 6 \left( 1 + \chi + \sqrt{1 + 14\chi + \chi^2} \right)^{-1}. \quad (8)$$

This result holds not only for a perpendicular shock but also for an oblique shock (see Eq.A14 in Komissarov & Lyutikov (2011)). Thus, the fraction of energy injected into PWN in the magnetic form along a wind streamline is

$$\delta_\alpha(\theta) = \chi_\alpha(\theta) \eta(\chi_\alpha(\theta)). \quad (9)$$

In the split monopole model the overall fraction of the wind power injected into PWN in the magnetic form is given by the integral

$$\langle \delta_\alpha \rangle = \frac{3}{2} \int_0^{\pi/2} \delta_\alpha(\theta) \sin^3 \theta d\theta. \quad (10)$$

The function  $\langle \delta_\alpha \rangle$  is shown in the left panel of Figure 1 and in Table 1. One can see that, unless the magnetic inclination is close to  $90^\circ$ , the fraction of magnetic energy is quite substantial. For the guide value of  $\alpha \simeq 45^\circ$  (Harding et al. 2008), we obtain  $\langle \delta \rangle \simeq 0.28$ . Thus, almost one third of the energy supplied into the Crab nebula can be in the magnetic form. The middle panel of Figure 1 shows how this flux is distributed over the polar angle for different magnetic inclinations. For  $\alpha < 50^\circ$  it peaks at the boundary of the striped zone, but for  $\alpha > 50^\circ$  the maximum is inside the striped zone.

#### 4 MAGNETIC DISSIPATION INSIDE THE NEBULA

The observed synchrotron and inverse-Compton emission of the nebula is well fitted by the ‘‘one-zone’’ model with magnetic field of strength  $B \simeq 125 \mu\text{G}$  (Meyer et al. 2010). Although the magnetic field in the nebula is unlikely to be uniform, this estimate is still more reliable than the usual equipartition one, which requires an additional assumption of parity between the energies of magnetic field and relativistic particles. The observed shape of the nebula can be described as a prolate spheroid with major and minor axes  $a = 4.4 \text{ pc}$  and  $b = 2.9 \text{ pc}$  (Hester 2008), which gives the volume  $V = (\pi/6)ab^2 \simeq 5.7 \times 10^{56} \text{ cm}^3$ . The corresponding total magnetic energy of the nebula is  $E_m = 3.5 \times 10^{47} \text{ erg}$ ,

which is significantly below the value of  $E_n$  we estimated in Sec.2.

Assuming parity between the energy of relativistic electrons emitting synchrotron radiation  $E_e$  and the magnetic energy  $E_m$ , Hillas et al. (1998) used the observed synchrotron luminosity of the nebula to derive its equipartition magnetic field  $B_{eq} = 330 \mu\text{G}$ . The lower value of  $B$  given by Meyer et al. (2010) suggests significant deviation from the energy equipartition. From the theory of synchrotron emission it follows that the total energy of emitting electrons

$$E_e \propto \frac{L_{\text{syn}}}{B^{3/2}} \left( \frac{\int_{\nu_{\text{min}}}^{\nu_{\text{max}}} n(\mathcal{E}) d\nu}{\int_{\nu_{\text{min}}}^{\nu_{\text{max}}} n(\mathcal{E}) \nu^{1/2} d\nu} \right),$$

where  $L_{\text{syn}}$  is the total synchrotron luminosity,  $n(\mathcal{E})$  is the electron energy spectrum, and  $\mathcal{E} \propto (\nu/B)^{1/2}$  is the characteristic energy of electron emitting at frequency  $\nu$  (Pacholczyk 1970). For a power-law spectrum the function in the brackets does not depend on  $B$  and thus  $E_e \propto B^{-3/2}$  with sufficient accuracy. Since  $E_m \propto B^2$  this leads to

$$E_e = E_m (B/B_{eq})^{-7/2}.$$

In the case of the Crab nebula this yields  $E_e \simeq 30E_m \simeq 1.0 \times 10^{49} \text{erg}$ , which is surprisingly close to our value of  $E_n$ , given the simplifications of the model.

This result suggests two possible explanations. First, the energy is indeed supplied into the nebula mainly in the form of relativistic particles. The analysis presented in the previous section shows that this would require the Crab pulsar to be almost an orthogonal rotator, in fact we would need  $\alpha \simeq 76^\circ$ . If however the magnetic inclination angle is indeed close to  $\alpha = 45^\circ$ , obtained in Harding et al. (2008) via modeling of the pulsed emission, then an efficient dissipation of magnetic field inside the nebula, accompanied by particle acceleration, is required to explain the data.

Assuming that a fraction  $\langle \delta \rangle$  of  $L_{sp}$  is supplied into the nebula in the magnetic form, one can find the characteristic timescale of this dissipation via balancing the supply and dissipation rates as

$$\tau_{md} = \frac{E_m}{\langle \delta \rangle L_{sp}} \simeq 80 \left( \frac{\langle \delta \rangle}{0.3} \right)^{-1} \text{ yr}. \quad (11)$$

This is much smaller compared to the dynamical timescale  $\tau_{dn} \simeq 950 \text{ yr}$ , which justifies the omission of adiabatic energy losses in this estimate. Moreover,  $\tau_{md}$  exceeds the light crossing time of the nebula,  $\tau_c \simeq 12 \text{ yr}$ , only by a factor of  $\sim 7$ . This shows that the magnetic dissipation is a very fast process. For example, the speed of magnetic energy supply into reconnection zones is likely to be limited from above by  $\sim 0.1$  of the Alfvén speed (Lyubarsky 2005), which in the relativistic MHD is

$$c_a = c \left( \frac{\tilde{\sigma}}{1 + \tilde{\sigma}} \right)^{1/2},$$

where  $\tilde{\sigma} = B^2/4\pi w$ , where  $w = \rho c^2 + \Gamma p/(\Gamma - 1)$  is the relativistic enthalpy and  $p$  is the gas pressure. In magnetically dominated plasma  $\tilde{\sigma} \gg 1$  and  $c_a$  is close to the speed of light, whereas in particle-dominated plasma with  $\tilde{\sigma} \ll 1$ , it can be significantly lower. The mean  $\tilde{\sigma}$  of the nebula can

be estimated as  $\langle \tilde{\sigma} \rangle \simeq 2E_m/E_e \simeq 0.07$  leading to the reconnection speed  $< 0.025c$ . If the reconnection flow had the form of a large-scale advection towards the equatorial plane and polar axis, like that proposed in Lyutikov (2010), the corresponding dissipation timescale would be  $\gtrsim 300 \text{ yr}$ , which seems too high compared to  $\tau_{md}$ . In order to reduce this timescale one would have to involve numerous simultaneously active reconnection sites throughout the volume of the nebula.

## 5 DISCUSSION

### 5.1 Magnetic dissipation and the fine structure of the Crab Nebula

The possibility of efficient magnetic dissipation in the Crab nebula raises the question about its observational signatures. What kind of structures if any should we expect to see and where? Unfortunately, our current understanding of magnetic reconnection is not that advanced to make any firm predictions. The most explored and firmly associated with magnetic reconnection phenomena in astrophysics are solar flares. They involve significant restructuring of magnetic fields anchored to the solar surface and distorted by motions in the Sun. It is not clear if such grand events may occur under the conditions of PWN. Smaller scale ‘‘nanoflares’’ could be responsible for heating of solar corona and the appearance of bright coronal loops (Parker 1972), but even this issue has not been settled yet. The so-called ‘‘reconnection exhausts jets’’ have been detected in the solar wind via in situ measurements using spacecrafts (see Gosling 2011, and references therein). These observations show no evidence of non-thermal particle acceleration or electron heating and do not allow to say how far a spacecraft is from a reconnection site or even if reconnection is still ongoing at the time of observation. Other examples include Earth’s magnetosphere and laboratory experiments but these seem to be too specific.

For the purpose of identifying the locations of magnetic dissipation in PWN, a non-thermal particle acceleration is its most promising and also likely product. This process could brighten up the interfaces between regions with different orientation of magnetic field. The polarimetric observations of the Crab Nebula by Bietenholz & Kronberg (1991) show that in its central region the degree of polarization is about 5 times below that for the synchrotron emission in uniform magnetic field. They explain this result by the presence along the line of sight of several cells with randomly oriented uniform magnetic field. Boundaries of such cells could be the sites of ongoing magnetic reconnection and may appear as arcs or filaments of enhanced nonthermal emission.

In fact, the Crab nebula has the most spectacular network of optical filaments but they are made of the line-emitting thermal plasma of the supernova ejecta ionized by the synchrotron radiation of the PWN. In the optical continuum, only the bright cores of these filaments can be seen and only as absorbing features (e.g. Fesen & Blair 1990; Sankrit et al. 1998). The radio emission of the Crab nebula has synchrotron origin and given the results of the optical continuum observations one would not expect to find the filaments in radio images of the nebula. To the contrary, the

high resolution VLA radio images do show filamentary structure which is as spectacular as that of the line emission maps (e.g. Bietenholz et al. 2004). Moreover, the radio filaments seem to coincide with the line-emitting optical filaments. This was noticed already in the early lower resolution study of the nebula with the Cambridge One-Mile radio telescope (Wilson 1972).

A localized enhancement of synchrotron emissivity does not have to be related to particle acceleration and may simply reflect a local enhancement of magnetic field. Such enhancement could well arise during interaction between the high speed flow of relativistic plasma inside the PWN with the filaments via the so-called “magnetic draping” effect (e.g. Lyutikov 2006). However, in this case one would generally expect the optical non-thermal emissivity to increase as well. Since this is not what is observed, other factors should come into play.

The origin of radio emitting electrons (and positrons) of the Crab nebula is a long standing mystery. The most natural assumption is that they come with the wind from the Crab pulsar just like the higher energy electrons, but their number seems to be too high to be accommodated in the current models of pair production in pulsar magnetospheres (Arons 2012). The radio observations of the inner Crab nebula could have settled this issue should they revealed the same features associated with the outflow from the termination shock as in optics and X-rays, or otherwise. Unfortunately, the emerging picture is rather ambiguous. Although radio wisps are observed, they do not coincide with the optical ones and are noticeably slower (Bietenholz et al. 2004). There is no obvious radio counterpart to the optical and X-ray jet either. Given the strong anisotropy of the pulsar wind, this may indicate that radio electrons and positrons come from different parts of the termination shock. On the other hand, the radio wisps could just be some kind of ripples driven by the unsteady outflow from the termination shock through the PWN. Indeed, the MHD simulations show strong convective motion inside the nebula which brings plasma from outer parts of the nebula quite close to termination shock, where it is pushed out again by the outflow from the termination shock (Camus et al. 2009).

The quantity of radio electrons may be large compared to what is expected in the theory of pulsar magnetospheres, but it is tiny compared to what is available in the line-emitting filaments. It is conceivable that a small fraction of the filament plasma becomes loose and mixes with the relativistic plasma of PWN. In there, its electrons can be accelerated to relativistic energies and produce the observed synchrotron radio emission. Kennel & Coroniti (1984) estimate the energy contained in the radio electrons to be of the order of few  $\times 10^{48}$  erg, which is a sizable fraction of the total internal energy of the nebula. Thus, in situ acceleration of radio electrons requires a substantial source of energy. This could be the energy of the magnetic field injected into the nebula by the pulsar wind, which can indeed be substantial, as we argued in Sec.3. The magnetic dissipation can be enhanced near the line-emitting filaments when magnetic field lines of different orientation wrap around the same filament. The magnetic reconnection could also facilitate escape of electrons (and ions) from the filaments into Crab’s PWN, otherwise suppressed by the low diffusivity across magnetic field lines. The other possibility is the second-order Fermi ac-

celeration by the hydromagnetic turbulence driven by various instabilities (Bucciantini et al. 2011). The existence of two synchrotron components of different origin is supported by the combined radio and mm-wavelength observations (Bandiera et al. 2002). The data suggest low energy cutoff around 100 GHz in the emission of the electrons supplied by the termination shock, thus supporting a different origin of radio emitting electrons. However, the relatively smooth matching of radio and optical/infrared components of the integral spectrum may be problematic for this model, particularly when seen in a number of PWN (Bucciantini et al. 2011).

Velusamy et al. (1992) state that the VLA images also show filaments which do not have line emitting counterparts. The spectral data do not show any noticeable variation of the radio spectral index across the filaments (Bietenholz et al. 1997). Since the synchrotron life-time of radio emitting electrons significantly exceeds the age of the nebula, this is not very surprising. Some of the filaments are also seen in the X-ray band (Seward et al. 2006). Since the life-time of X-ray emitting electrons is quite short, one would expect to see hardening of the X-ray spectrum of the filaments compared to the diffuse background if these filaments were indeed the sites of particle acceleration. However, the observations give no evidence of such hardening and the photon index is very soft,  $\alpha \sim 3 - 4$  (Seward et al. 2006), creating a problem for any model where these features act as acceleration sites of electrons emitting in X-rays (Seward et al. 2006).

The continuum optical images of the Crab nebula reveal fine fibrous structure somewhat reminiscent of solar coronal loops (Fesen & Blair 1990; Hester et al. 1995). However, it is not clear if this is a product of “nanoflares” or simply reflects inhomogeneous structure of magnetic field.

## 5.2 Implications for numerical simulations of PWN

The 2D RMHD numerical simulations of the Crab nebula (Komissarov & Lyubarsky 2003; Del Zanna et al. 2004; Bogovalov et al. 2005; Camus et al. 2009) have been very successful in reproducing many key properties of the nebula, such as its jet-torus, the brightness asymmetry, wisps, and even the bright “inner knot” (Hester et al. 1995). In agreement with the observations, the proper motion of jets and wisps produced in the simulations is relatively low,  $v = 0.2 - 0.7c$ , as expected downstream of an almost purely hydrodynamical shock wave. This success leaves little doubt that the numerical models capture the physics of the nebula quite well.

However, the overall low wind magnetization utilized in these models,  $\langle \sigma \rangle \simeq 10^{-2}$ , is in conflict with what we would expect in the striped wind model without imposing very large magnetic inclination angle of the pulsar. This choice of  $\sigma$  has been influenced by the very low value required in the Kennel-Coroniti model in order to have a termination shock in their 1D solution. However, the flow dynamics of the 2D numerical solutions is already very different, as it involves large scale circulation and mixing. Although Komissarov & Lyubarsky (2004) did find that, in qualitative agreement with predictions of the Kennel-Coroniti model, the size of the termination shock decreased with  $\langle \sigma \rangle$ , no attempts have been made to study models with  $\sigma \gg 10^{-2}$ . As the

result, one cannot claim yet that 2D numerical simulations rule them out. As the shock size is determined by the balance between the wind ram pressure and the total pressure in the nebula, this tendency can be explained by the stronger axial compression of the nebula by the magnetic hoop stress in models with higher  $\sigma$ . However, this compression is certainly excessive in 2D models, being enforced by the condition of axial symmetry which does not allow development of the kink instability (Begelman 1998). The 3D numerical study of z-pinch configurations by Mizuno et al. (2009, 2011) confirms this expectation. Thus, the ultimate answer to the question whether  $\langle \sigma \rangle \gg 10^{-2}$  is allowed by the RMHD model will only be found in future 3D simulations of PWN.

If at high latitudes the pulsar wind is free from stripes and has high  $\sigma$  then downstream of the termination shock one would expect a very fast flow, with the Lorentz factor  $\gamma \sim \sigma^{1/2}$  in the case of perpendicular shock (Kennel & Coroniti 1984a) and even higher in the case of oblique shock (Komissarov & Lyutikov 2011). Downstream of a perpendicular shock the flow is subsonic (or sub-fast-magnetosonic to be more precise) and can smoothly decelerate down to  $\gamma \simeq 1$  inside the nebula. Downstream of an oblique shock it may remain supersonic and a secondary shock will have to appear somewhere on its way. So far the observations of the Crab nebula show no evidence of such a secondary shock or such a fast flow. This may well be related to the low dissipation efficiency of shocks in highly magnetized plasma (e.g. Kennel & Coroniti 1984a; Komissarov 2012), as well as the inability of such shocks to accelerate non-thermal particles (Sironi & Spitkovsky 2009, 2011a). Further investigation is required to clarify this issue.

### 5.3 Magnetic dissipation and Crab’s gamma-ray flares

The recently discovered strong flares of gamma-ray emission from the Crab nebula at the energies  $\sim 1$  GeV with duration about few days (Tavani et al. 2011; Abdo et al. 2011) could be very important for understanding the physics of highly magnetized relativistic plasma. Komissarov & Lyutikov (2011) argued that the gamma-rays of these energies could originate from the most compact known bright feature of the Crab nebula, the so-called “inner knot”, which they explain as a Doppler-boosted emission from the termination shock. However, their model predicts synchronous variability of the knot emission in gamma-rays and optics, which does not seem to be the case (Arons 2012). The only other promising alternative seem to be explosive magnetic reconnection.

However, the properties of these flares suggest that they may not be representative of the energetically dominant magnetic dissipation process in the nebula. First, the dissipation time scale given by Eq.11 is at least three orders of magnitude longer than the typical flare duration. It is possible that the tearing instability produces much smaller structures inside the large scale current sheets, however in this case one would expect a whole spectrum of time scales to be present. Second, the statistical model of flares by (Clausen-Brown & Lyutikov 2012) gives the total energy release rate which is three orders of magnitude below the spindown power of the Crab pulsar and hence significantly lower than the magnetic dissipation rate given by Eq.11.

Third, the current reconnection models of these flares involve strong magnetic fields, of order  $1000 \mu\text{G}$  (Uzdensky et al. 2011; Cerutti et al. 2012), and/or large bulk Lorentz factors  $\Gamma \gtrsim \text{few}$  (Komissarov & Lyutikov 2011; Clausen-Brown & Lyutikov 2012). Such conditions are not typical for the Crab nebula. Finally, so far the flares have not been identified with any particular kind of events seen at other energies.

Given the required conditions for the flares, their most likely location is the polar region near the termination shock, where the freshly supplied plasma can have very high magnetization and streams with ultra-relativistic speeds<sup>2</sup>. Large Lorentz factors could also be produced during fast reconnection events inside high- $\bar{\sigma}$  plasma, which again points out towards the inner polar region of the Crab nebula, where the observations reveal the Crab jet. High magnetization also implies Alfvén speed approaching the speed of light and hence the fastest possible magnetic reconnection speed. Cerutti et al. (2012) also point out that magnetic field in this region can be much stronger than on average due to the strong axial compression associated with the z-pinch. The region at the base of the Crab jet, the so-called “anvil”, is in fact the most active region in the nebula (Hester et al. 2002).

## 6 SUMMARY

(i) We have calculated the power of high- $\sigma$  striped pulsar wind which remains as the Poynting flux after total dissipation of its stripes in the split-monopole approximation. The results show that the pulsar has to be an almost exact orthogonal rotator for the mean wind  $\sigma$  to reduce down to the very low values suggested by the Kennel-Coroniti model (and to some degree by the current axisymmetric numerical models of the Crab nebula). For the more realistic magnetic inclination angle  $\alpha \simeq 45^\circ$ , about 30 percent of the wind power is retained in the form of the Poynting flux. While low magnetization is achieved in the equatorial plane, in the polar zone the magnetization remains very high.

(ii) Given the relatively long spindown time of the Crab pulsar and low radiative losses, we find that out of  $E \simeq 3.7 \times 10^{49}$  erg of energy that has been supplied by the pulsar wind into the nebula  $E_n \simeq 1.3 \times 10^{49}$  erg should still remain as its internal energy, sheared between magnetic field and relativistic particles.

(iii) The observations of synchrotron and inverse-Compton emission of the Crab nebula indicate that most of  $E_n$  is stored in relativistic electrons and positrons, and only  $E_m \simeq 3.5 \times 10^{47}$  erg in the magnetic field. This may be simply down to the fact that from the start the energy is injected into the nebula mostly in the form of relativistic particles. In the striped wind model, this would imply that the Crab pulsar is almost an exact orthogonal rotator. Alternatively, most of the injected magnetic energy may have been dissipated and transferred to the particles via magnetic reconnection events.

<sup>2</sup> A similar conclusion was reached recently by Y. Lyubarsky at a conference presentation ([http://www.iasf-roma.inaf.it/Flaring\\_Crab/index.html](http://www.iasf-roma.inaf.it/Flaring_Crab/index.html)).

(iv) Using the magnetic inclination angle of the Crab pulsar derived from modeling of its high energy pulsed emission,  $\alpha = 45^\circ$ , we estimate the characteristic timescale of magnetic dissipation in the Crab nebula to be  $\tau_{md} \sim 80$  yr. This relatively short timescale implies complex structure in the magnetic field distribution inside the nebula, which is supported by the radio and optical observations.

(v) Since the scale of deduced magnetic dissipation inside the Crab nebula strongly depends on the magnetic inclination angle of its pulsar, accurate observational measurements of this angle would be very important. A search for signs of ongoing magnetic dissipation, such as particle acceleration inside the nebula, is another important direction of observational studies. It seems plausible that the observed enhanced radio emissivity in vicinity of line-emitting filaments is a result of magnetic dissipation.

(vi) The recently discovered gamma-ray flares may be the first strong indication of magnetic reconnection inside the Crab nebula. However, their short timescale, low energetics, and extreme conditions requires in the current theoretical models suggest that these events may not be representative of the dominant magnetic dissipation process in the nebula.

## ACKNOWLEDGMENTS

We thank Y.Lyubarsky for careful reading of the manuscript and finding an error in the original derivations as well as the anonymous referee for numerous suggestions on improving the presentation. This research was funded by STFC under the standard grant ST/I001816/1.

## REFERENCES

- Arons, J., 2012, *Sp.Sci.Rev.*, in press.
- Abdo, A. A. et al. (The Fermi Collaboration), 2011, *Science*, 331, 739
- Bandiera, R., Neri, R., Cesaroni, R., 2002, *A&A*, 386, 1054
- Begelman, M. C., 1998, *ApJ*, 493, 291
- Begelman, M. C., Li, Z.-Y., 1992, *ApJ*, 397, 187
- Bietenholz, M. F., Kronberg, P. P., Hogg, D. E., Wilson, A. S., 1991, *ApJ*, 373, L59
- Bietenholz, M. F., Kronberg, P. P., 1991, *ApJ*, 368, 231
- Bietenholz, M. F., Kassim, N., Frail, D. A., Perley, R. A., Erickson, W. C., Hajian, A. R., *ApJ*, 490, 291
- Bietenholz, M. F., Hester, J. J., Frail, D. A., Bartel, N., 2004, *ApJ*, 615, 794
- Bogovalov, S. V., 1999, *A&A*, 349, 1017
- Bogovalov, S. V., Chechetkin, V. M., Koldoba, A. V., Ustyugova G. V., 2005, *MNRAS*, 358, 705
- Bucciantini, N., Arons, J., Amato, E., 2011, *MNRAS*, 410, 381
- Camus, N. F., Komissarov, S. S., Bucciantini, N., Hughes, P. A., 2009 *MNRAS*, 400, 1241
- Cerutti, B., Uzdensky, D. A., Begelman, M. C., 2012, *ApJ*, 746, 148
- Clausen-Brown, E., Lyutikov, M., 2012, *MNRAS*, in press (arXiv1205.5094)
- Coroniti, F. V., 1990, *ApJ*, 349, 538
- Drenkhahn G., Spruit H. C., 2002, *A&A*, 391, 1141
- Del Zanna, L., Amato, E., Bucciantini, N., 2004, *A&A*, 421, 1063
- Emmering, R. T., Chevalier, R. A., 1987, *ApJ*, 321, 334
- Fesen, R. A., Blair, W. P., 1990, *ApJ*, 351, L45
- Giannios, D., 2011, *J.Phys: Conf.Series*, 283, 012015
- Gosling, J. T. 2011, *Space Sci Rev*, 1, 14
- Harding, A. K., Stern, J. V., Dyks, J., Frackowiak, M., 2008, *ApJ*, 680, 1378
- Hester, J. J., et al., 1995, *ApJ*, 448, 240
- Hester J. J., et al., 2002, *ApJL*, 577, L49
- Hester J. J., 2008, *Ann.Rev.Astron.Astrophys.*, 46, 127
- Hillas, A. M. et al., 1998, *ApJ*, 503, 744
- Kalapotharakos, C., Contopoulos, I., 2009, *A&A*, 496, 495
- Kennel, C. F., Coroniti, F. V., 1984a, *ApJ*, 283, 694
- Kennel, C. F., Coroniti, F. V., 1984b, *ApJ*, 283, 710
- Komissarov, S.S., 2011, *Memorie della Societa Astronomica Italiana*, 82, 95
- Komissarov, S. S., 2012, *MNRAS*, 422, 326
- Komissarov, S. S., Lyubarsky, Y. E., 2003, *MNRAS*, 344, L93
- Komissarov S. S., Lyubarsky Y. E., 2004, *MNRAS*, 349, 779
- Komissarov, S. S., Lyutikov, M., 2011, *MNRAS*, 414, 2017
- Komissarov S. S., Vlahakis N., Königl A., Barkov M. V., 2009, *MNRAS*, 394, 1182
- Lyne, A. G., Pritchard, R. S., Smith F. G., 1993, *MNRAS*, 265, 1003
- Lyubarsky Y. E., 2002, *MNRAS*, 329, L34
- Lyubarsky Y.E., 2003a, *MNRAS*, 339, 765
- Lyubarsky Y. E., 2003b, *MNRAS*, 345, 153
- Lyubarsky Y. E., 2005, *MNRAS*, 358, 113
- Lyubarsky Y. E., 2010, *MNRAS*, 402, 353
- 2011, *Phys.Rev.E*, 83, 6302
- Lyubarsky Y. E., Kirk, J. D., 2001, *ApJ*, 547, 437
- Lyutikov M., Blandford R. D., 2003, *astro-ph/0312347*
- Lyutikov, M., 2006, *MNRAS*, 373, 73
- Lyutikov, M., 2010, *MNRAS*, 405, 1809
- McKinney J.C., Uzdensky D.A., 2012, *MNRAS*, 419, 573
- Meyer, M., Horns, D., Zechlin, H.-S., 2010, *A&A*, 523, 2
- Mizuno, Y., Lyubarsky, Y., Nishikawa, K.-I., Hardee, P. E., 2009, *ApJ*, 700, 684
- Mizuno, Y., Lyubarsky, Y., Nishikawa, K.-I., Hardee, P. E., 2011, *ApJ*, 728, 90
- Parker, E. N., 1972, *ApJ*, 107, 499
- Pacholczyk, A.G., *Radio Astrophysics: Nonthermal Processes in Galactic and Extragalactic Sources*, W. H. Freeman & Co Ltd, 1970
- Rees, M. J., Gunn, J. E., 1974, *MNRAS*, 167, 1
- Sankrit, R., 1998, *ApJ*, 504, 344
- Sironi, L., Spitkovsky, A., 2009, *ApJ*, 698, 1523
- Sironi, L., Spitkovsky, A., 2011a, *ApJ*, 726, 75
- Sironi, L., Spitkovsky, A., 2011b, *ApJ*, 741, 39
- Spitkovsky, A., 2006, *ApJ Lett.*, 648, L51
- Seward, F. D., Tucker, W. H., Fesen, R. A., 2006, *ApJ*, 652, 1277.
- Tavani, M., et al. 2011, *Science*, 331, 736
- Trimble, V., 1968, *Astron.J.*, 73, 535
- Velusamy, T., Roshi, D., Venugopal, V. R., 1992, *MNRAS*, 255, 210
- Vlahakis N., Königl A., 2004, *ApJ*, 605, 656
- Uzdensky, D. A., Cerutti, B., Begelman, M. C., 2011, *ApJ Lett.*, 737, L40



Wilson, A. S., 1972, MNRAS, 157, 229  
Wyckoff, S., Murray, C. A., 1977, MNRAS, 180, 717  
Zhang B., Yan H., 2011, ApJ, 726, 90